Solubilization and Reconstitution of Vesicular Stomatitis Virus Envelope Using Octylglucoside

M. Paternostre,* M. Viard,* O. Meyer,* M. Ghanam,* M. Ollivon,* and R. Blumenthal#
*Equipe "Physicochimie des Systèmes Polyphasés," URA CNRS 1218, Université Paris Sud, 92296 Châtenay Malabry, France, and #National Institutes of Health/National Cancer Institute, Laboratory of Mathematical Biology, Bethesda, Maryland 20892, USA

ABSTRACT Reconstituted vesicular stomatitis virus envelopes or virosomes are formed by detergent removal from solubilized intact virus. We have monitored the solubilization process of the intact vesicular stomatitis virus by the nonionic surfactant octylglucoside at various initial virus concentrations by employing turbidity measurements. This allowed us to determine the phase boundaries between the membrane and the mixed micelles domains. We have also characterized the lipid and protein content of the solubilized material and of the reconstituted envelope. Both G and M proteins and all of the lipids of the envelope were extracted by octylglucoside and recovered in the reconstituted envelope. Fusion activity of the virosomes tested either on Vero cells or on liposomes showed kinetics and pH dependence similar to those of the intact virus.

INTRODUCTION

An important problem in the delivery of drugs and other agents into cells is the passage of permeability barriers imposed by the cell plasma membranes (Blumenthal, 1987). Enveloped viruses have developed a "Trojan horse" strategy to circumvent such barriers. These viruses inject their genetic content into the cytoplasm of the host cell after fusion between the viral and cellular membranes (Marsh and Helenius, 1989). Strategies have been developed for in vitro and in vivo use of the viral envelope as a Trojan horse (Blumenthal and Loyter, 1991). This involves disassembly of the virus by detergent, followed by reassembly of its envelope to repackage the materials to be delivered into cells.

The attachment of the viral particles to the cell surface is mediated by the viral glycoproteins that constitute the spikes in the viral envelope and specifically recognize cellular receptors for the virus present in the plasma membrane of the target cell (Lenard, 1990; Blumenthal et al., 1994; Gaudin et al., 1995a). Significant advances have been made in recent years in the knowledge of the sequences and structure of viral envelope proteins, and genetic and chemical methods have been developed for site-specific alterations (White, 1992; Schoch and Blumenthal, 1993). However, little is known about the sequence of molecular events involved in the membrane fusion mediated by the viral envelope proteins. Kinetic assays for the fusion of fluorescently labeled virus with a variety of target membranes have been developed using spectrofluorometric (Struck et al., 1981; Hoekstra et al., 1984; Blumenthal et al., 1987; Clague et al., 1990) and video microscopic techniques (Paternostre et al., 1989; Blumenthal et al., 1995; Zimmerberg et al., 1994; Sarkar et al., 1989). Fusion of viral envelopes with cell membranes has been studied by using those assays with a variety of different virus strains, which include those that enter cells by acid-activated fusion after endocytosis (Puri et al., 1993a). It is possible to continuously monitor fluorescence changes before and during fusion with diverse target membranes (Lorge et al., 1986; Stegmann et al., 1989; Puri et al., 1992a,b, 1993b; Wilschut et al., 1995; Gaudin et al., 1993). The results yield insights into the complexity of the fusion process. With these methods the fusion characteristics of reconstituted virus envelope are compared to those of intact virus as an indicator of successful reconstitution (Eidelman et al., 1984; Paternostre et al., 1989; Bron et al., 1993; Hug and Sleight, 1994).

Reconstituted viral envelope proteins must be able to induce fusion between membranes in a biologically relevant manner. This requires part of the fusion proteins to be anchored and oriented in the reconstituted membrane in a fashion similar to what it was in the original viral envelope. In many cases, one or more auxiliary proteins are required in addition to the viral fusion protein. Detergents solubilize natural membranes by intercalating among the phospholipids until the mole fraction of detergent is so high that the mixture no longer forms a bilayer (Meyer et al., 1992; de Foresta et al., 1990). Ideally, the structure of the protein-detergent micelle will be such that the membrane-spanning regions of the protein are protected from the aqueous environment, without disrupting the structure of the extramembraneous portions. Most of the time, empirical formulae are used to ensure an excess of detergent for solubilization without denaturing the protein. The solubilized proteins of interest are purified, and components (lipids, protein, lipid or aqueous labels, and material to be encapsulated) can be added. Reconstitution is achieved by reversing the solubilization process to form viral envelopes. When the detergent concentrations limiting the solubility of lipid and protein are similar, the detergent-lipid and detergent-protein mixed micelles coalesce into multicomponent micelles, then into

Received for publication 5 August 1996 and in final form 26 November 1996.

Address reprint requests to Dr. Maite Paternostre, Equipe "Physiochimie des Systèmes Polyphasés," URA CNRS 1218, Université Paris Sud, 5 rue J. B. Clement, 92296 Chatenay-Malabry Cedex, France. Tel.: 33-01-4683-5644; Fax: 33-01-4683-5312; E-mail: paternos@cep.u-psud.fr.

0006-3495/97/04/1683/12 $2.00

sheets or fragments of membrane, which subsequently close to form vesicles. In principle, the molecular rearrangements that occur during detergent removal follow the same pathway as during the solubilization. Usually, however, the supramolecular arrangement obtained after detergent removal is different from the initial one. The more difficult characteristics to reproduce are the asymmetrical orientation of the protein and the asymmetrical distribution of the lipids that may exist in the natural membrane. Moreover, the type of reconstituted vesicle formed depends dramatically on the conditions of detergent removal (Eytan, 1982; Walter et al., 1988). Inappropriate reconstitution will lead to the formation of vesicles without protein, together with protein-rich aggregates.

Although a large number of viral spike glycoproteins have already been incorporated into lipid vesicles (Petri and Wagner, 1979; Miller et al., 1980; Petri and Wagner, 1980; Pal et al., 1983; Metsikkö et al., 1986; Paternostre et al., 1989; Hug and Sleight, 1994), it has been shown only in a few cases that the reconstituted product was functionally active in the same way as intact virus in inducing membrane fusion (Vainstein et al., 1984; Nussbaum et al., 1987; Lapidot et al., 1987; Stegmann et al., 1987; Paternostre et al., 1989). A method has been developed to form functional reconstituted viral envelope from Sendai virus, influenza virus, and vesicular stomatitis virus. The procedure involves extraction of the envelope by Triton X-100 followed by detergent removal by the direct addition of SM2 biobeads (BB SM2). Few attempts have been made to mediate viral glycoprotein reconstitution using the nonionic detergent octylglucoside (OG) (Metsikkö et al., 1986), but most of the time they resulted in nonactive preparation. In numerous cases, OG is used to extract the glycoprotein, and thereafter it is replaced by another detergent (i.e., Triton X-100) before reconstitution or eliminated for direct reconstitution into preformed liposomes (Hug and Sleight, 1994). However, OG would present numerous advantages compared to Triton X-100:

1. Because of its high critical micellar concentration (CMC), OG removal is easily achieved and monitored by different techniques like BB SM2 treatment, but also by dialysis and by dilution.

2. OG has also been shown to promote massive vectorial incorporation of membrane proteins into preformed liposomes, if the latter have been pretreated with nonsolubilizing concentration of OG (Paternostre et al., 1988; Rigaud et al., 1988, 1995).

In the present work we report a systematic study of the solubilization of vesicular stomatitis virus (VSV) by OG. From these experiments we have determined precisely the relations between OG and VSV concentrations along the solubilization process. We show that when the minimum OG concentration required for total solubilization of the viral envelope is used, and after detergent removal by BB SM2 treatment, the pH-dependent fusion activity of the reconstituted system is comparable to that of the intact virus. At each step of the solubilization and reconstitution processes, lipids and proteins were assayed to determine which component of the virus interacts with the detergent. The final virosomes contain G and M proteins together, and all of the lipids in ratios similar to those of the initial envelope. Fusion kinetics have been recorded using either Vero cells and octadecyl rhodamine-labeled virosomes or virosomes and liposomes labeled with *N*-(7-nitro-2,1,3-benzoxiadiazol-4-yl)phosphatidylethanolamine (NBD-PE) and *N*-(lissamine rhodamineB sulfonyl) phosphatidyl-ethanolamine (Rho-PE), as described for rabies virus by Gaudin et al. (1993). The orientation of the fusogenic protein has not been tested, but the fusion activity tests indicate that part of this protein is well oriented in the reconstituted system.

MATERIALS AND METHODS

Materials

OG was obtained from Sigma; 8-anilinophtalene-1-sulfonate (ANS) was obtained from SERVA; BB SM2 were purchased from BioRad; Octadecyl rhodamine (R18) was purchased from Molecular Probes; NBD-PE and Rho-PE were from Avanti; and egg phosphatidylcholine (EPC), egg phosphatidylethanolamine, and gangliosides (type III) extracted from bovine brain (Gang) were from Sigma. The cholesterol and phospholipid assay kits were obtained from Biomerieux (Marcy l'Etoile, France). The protein assay was purchased from BioRad.

Virus cultures

Virus (Indiana) was grown on monolayer cultures of baby hamster kidney (BHK-21) cells and purified by sucrose velocity and density gradients to approximately 1 mg/ml of VSV protein per milliliter (Newcomb et al., 1982). The sucrose gradient solutions were made in a buffer containing 10 mM Tris, 1 M NaCl, and 1 mM EDTA (pH 7.5). ^{3}H-labeled VSV was prepared by infecting BHK cells in the presence of [^{3}H]leucine (5 mCi/ml growth medium). The specific activity ranged from 200 to 2000 cpm/mg VSV protein. The purified virus was stored at −70°C in the buffer described above and containing about 30% (W/V) sucrose.

Before use, the VSV were dialyzed against a sucrose-free medium containing 1 M NaCl, 1 mM EDTA, 10 mM HEPES (pH 7.5). In some cases, VSV was labeled with R_{18}, as described by Blumenthal et al. (1987), from an ethanolic solution to reach a probe-to-lipid ratio of about 1%. The nonincorporated probe was eliminated by gel exclusion chromatography using a PD10 column (Pharmacia).

Cell culture

Vero cells were grown to confluence in a Dulbecco's minimum essential medium supplemented with 10% calf serum in 75-cm^2 plastic dishes. The fusion experiments were carried out with the cells in suspension. The cells were incubated for 10 min at 37°C in 1 ml phosphate-buffered saline medium containing 0.5 mg trypsin and 0.2 mg EDTA, yielding 2×10^7 cells/ml. Before the experiments the cells were washed three times by centrifugation in a solution containing 10 mM HEPES and 145 mM NaCl, pH 7.4, to remove trypsin from the cells in suspension.

Liposomes

Liposomes consisting of egg phosphatidylcholine, phosphatidylethanolamine, and gangliosides in a weight ratio of 1/2/0.5 and labeled with the fluorescence energy transfer pair NBD-PE and Rho-PE were obtained by sonication. A stock chloroformic solution of the lipid mixture containing 1% (w/w) of each probe was prepared. The chloroform was evaporated,

and the dried lipid film was hydrated with a buffer solution (10 mM HEPES, 145 mM NaCl, pH 7.4) to get a final lipid concentration of about 1 mg/ml. After vortex mixing, the lipid suspension was submitted to sonication using a Vibracell sonifier (Sonics and Material Corp.) at power level 2 for six cycles of 2-min burst at 1-min intervals under nitrogen atmosphere and in an ice bath to maintain the sample at a temperature around 5°C. The sonicated material was centrifuged for 10 min at 9000 × g to remove titanium probe particles and passed through a 0.22-μm Millex filter. The resulting liposomes had an average diameter of 100 nm, as measured by quasi-elastic light scattering (QELS) with an N4 (Coultronics).

Methods

Determination of the CMC of OG

Different saline buffers ([HEPES] = 10 mM and 0 < [NaCl] < 1 M, pH 7.4) containing 1 μM ANS were prepared. The ANS fluorescence (λ_{ex} = 380 nm, λ_{em} = 490 nm) was recorded on a spectrofluorimeter SPEX (FILIII) connected to a computer. The buffer containing the ANS was poured directly into a quartz cuvette, which was placed in the spectrophotometer, maintained under gentle and continuous stirring, and thermostatted at 25°C (± 0.2°C). The evolution of ANS fluorescence was continuously monitored during the addition of a concentrated OG solution (200 mM). The rate of OG addition was controlled by a syringe pump (Perfusor VI; Braun). The OG concentration in the cuvette was then calculated from the time using the following equation:

$$[OG]_{tot} = ([OG]_s * r_s * t)/(v_o + (r_s * t)) \quad \text{(mM)}, \qquad (1)$$

in which $[OG]_s$ is the OG concentration in the syringe in mM, $[OG]_{tot}$ is the OG concentration raised in the cuvette at any time in the experiment, r_s is the injection rate of the syringe pump in ml/min, t is the time in min, and v_o is the initial volume in the cuvette in ml. The CMC of OG in the buffer used was then graphically determined by the intercept of the tangents, as indicated in Fig. 1.

Solubilization of VSV

The solubilization of intact viruses has been followed during the continuous addition of OG by measuring optical density (OD) at 550 nm on a Perkin-Elmer (Lambda 2) double-beam spectrophotometer. A volume of 1.4 ml of initial VSV solution was placed in a 1-cm optical quartz cell thermostatted at 25°C (±0.2°C) and equipped with a paddle stirrer. A concentrated OG solution made in the same buffer as the one used to dilute VSV (i.e., 1 M NaCl, 10 mM HEPES, 1 mM EDTA, pH 7.4) was progressively added through thin tubing connected to a glass precision syringe pump (Perfusor VI; Braun). The OD was recorded as a function of time; this was related to the OG and VSV concentrations in the cuvette by Eqs. 1 (see above) and 2, respectively:

$$[VSV]_{tot} = \frac{[VSV]_0}{1 + ([OG]_{tot}/([OG]_s - [OG]_{tot})} \quad \text{(mM)}, \qquad (2)$$

in which $[VSV]_0$ is the initial VSV concentration in the cuvette, which can be expressed in mg total protein/ml; $[VSV]_{tot}$ is the VSV concentration in the cuvette at any time in the experiment.

Removal of the nucleocapsid

The solubilized VSV was centrifuged for 1 h at 64,000 × g to spin down the nucleocapsid. The supernatant containing the solubilized proteins and lipids was collected.

Reconstitution of VSV envelope by dilution

The reconstitution profiles were obtained by following the turbidity (OD at 550 nm) at 25°C (± 0.2°C) during the continuous addition of free OG buffer to a cuvette containing 1 ml of the solubilized envelope. A volume of 2.5 ml of buffer was added to the cuvette over 3 h, giving a final dilution factor of 3.5. The OG and VSV concentrations were calculated from the time using Eqs. 3 and 4:

$$[OG]_{tot} = [OG]_0 * (v_0)/(v_0 + (r_s * t)) \quad \text{(mM)} \qquad (3)$$

$$[VSV]_{tot} = \frac{[VSV]_0 * v_0)}{(v_0 + (r_s * t) \quad \text{(mg of protein/ml)},} \qquad (4)$$

in which $[OG]_0$ and $[VSV]_0$ are the initial OG and VSV concentrations in the cuvette in mM and mg/ml, respectively; $[OG]_{tot}$ and $[VSV]_{tot}$ are the OG and VSV concentrations raised in the cuvette at any time in the experiment; r_s is the injection rate of the buffer in ml/min; t is the time in min; and v_0 is the initial volume in the cuvette in ml.

Reconstitution of VSV envelope by absorption of OG on BB SM2

For functional reconstitution, BB SM2 were used to eliminate OG. Ten vials were prepared, each containing 20 mg wet BB SM2 for each milliliter of sample. The sample was added to the first vial and kept under gentle magnetic stirring for 12 min at room temperature (25°C). Thereafter, the sample was taken from the vial and poured into the following vial. The total duration of the elimination is about 2 h. When needed, R18 was added to the solubilized sample at a probe-to-lipid ratio of 1% before detergent removal by BB SM2.

Radioactivity measurements

To set up these elimination conditions, [^{14}C]OG and [^{3}H]VSV were used to follow OG elimination and eventual protein absorption, respectively. The measurements have been made simultaneously on samples containing the two radiolabeled molecules, i.e. [^{14}C]OG and [^{3}H]leucine containing proteins, using a Beckman (LS 6000TA) liquid scintillation counter.

Activity assay

Fusion activities of intact virus and virosomes were tested either on Vero cells with R18-labeled viruses and/or virosomes, or on labeled NBD-PE and Rho-PE liposomes using nonlabeled viruses and/or virosomes.

Fusion activity measured on Vero cells. Fusion of R18-labeled viruses with Vero cells was carried out as described by Blumenthal et al. (1987). For fusion of R18-labeled virosomes with Vero cells, the procedure used was similar to the one described by Paternostre et al. (1989) for virosomes obtained by the elimination of Triton X-100. Before fusion assay, the virosomes were filtered through a 0.22-μm Millipore filter to remove aggregated virosomes. Then Vero cells and filtered virosomes were incubated at 4°C, under gentle stirring to allow the binding of virosomes to the cell surface. The Vero cell-virosome complexes were spun down and washed three times to remove the unbound virosomes. Then 20–30 μl of the complex was added to the buffer solution contained in a quartz cuvette, and maintained at 37°C under gentle magnetic stirring. The fluorescence of R_{18} (λ_{exc} = 565 nm, λ_{em} = 590 nm) was continuously recorded. After a 30-s wait for temperature equilibration, the pH solution was abruptly lowered to the desired pH value by adding aliquots of citric acid solution (0.1 M). The kinetics of R_{18} dequenching were followed for 3–5 min. The total fluorescence was estimated after the addition of a large amount of OG, and the percentage of fluorescence dequenching (%DQ) was determined by using Eq. 5:

$$\%DQ = ((F_{max} - F_f)/(F_{max} - F_o)) \times 100, \qquad (5)$$

in which F_{max} is the maximum fluorescence of the sample reached after solubilization by OG, F_f is the fluorescence reached at the end of the fusion kinetics, and F_o is the initial fluorescence of the Vero cell-virosome complexes. The pH was measured on each sample at the end of the fusion experiment.

Fusion activity measured on labeled liposomes. The fusion assays for intact viruses were carried out as described by Gaudin et al. (1993) for rabies viruses. Two milliliters of buffer solution were added to a quartz cuvette, thermostatted at the desired temperature, and maintained under gentle continuous magnetic stirring. When the temperature was stable, 10 μl of labeled liposomes (at 1 mg of lipids/ml) and 20 μl of VSV (at 1 mg of protein/ml) were added to the cuvette (unless other volumes are given in the text). Thereafter, evolution with time was recorded simultaneously for the fluorescence intensities at 530 nm and 590 nm (λ_{exc} = 470 nm). The pH was lowered by the injection of aliquots of citric acid (0.1 M) to the cuvette, and the fluorescence energy transfer was followed for 250 s after the pH change. The pH was measured at the end of the experiment, and the percentage of fluorescence increase at 530 nm was determined by using the maximum signal obtained after solubilization by OG and using Eq. 5.

The procedure was similar for virosomes. As the fluorescent probes were located in the liposomes, no difference in the extent of fluorescence increase was recorded, whether the virosomes were filtered or not. However, as the reconstitution procedure induced some loss of proteins (Table 2), the quantity of virosomes used to follow fusion was higher than in the case of intact viruses and adapted for each experiment.

Electrophoresis

Electrophoresis were carried out at each step of the solubilization and reconstitution processes to determine qualitatively the protein composition of the resulting virosomes. They were performed with mini-cell and precast 12% Tris-glycine gels (Novex; Prolabo France, Fontenay sous Bois, France). The samples were all pretreated by the same OG concentration to solubilize in the same condition all of the virus and virosome components. They were denatured at 95°C using β-mercaptoethanol and sodium dodecyl sulfate (SDS) solutions. Twenty-five microliters of each sample was layered on the gel. After migration, the protein bands were stained with Coomassie blue. A systematic scan of the gels was made after staining.

Protein assay

The total protein was assayed before and after solubilization, after centrifugation, and after reconstitution to check any loss of protein. For this we used the BioRad assay, based on classical Lowry procedure. The samples were completely solubilized by OG 200 mM before the assay, and the calibration curves were performed in the presence of the same amounts of OG. No perturbation of the assay coming from the presence of OG was detected.

Lipid assay

The lipids, particularly phosphatidylcholine and sphingomyelin on one hand and cholesterol on the other, were systematically assayed before solubilization, after solubilization, after centrifugation, and after reconstitution to check for any loss of lipids. The lipid assays were carried out using Biomerieux (Marcy l'Etoile, France) kits (Phospholipide enzymatique (PAP) and Cholesterol enzymatique (PAP150), for choline and cholesterol determinations, respectively), based on enzymatic specific reactions. Before the assays, the samples were completely solubilized by OG 200 mM, and the calibration curves were realized in the presence of the same amounts of OG. No perturbation of the assay due to the presence of OG was detected.

RESULTS

Solubilization of intact VSV by OG

VSV was stored in 10 mM Tris buffer at pH 7.4 containing 1 mM EDTA, 1 M NaCl, and 30% sucrose (876 mM). Before solubilization, we removed sucrose from the VSV suspension by dialysis against a sucrose-free buffer consisting of 1 M NaCl, 10 mM HEPES, and 1 mM EDTA.

Despite the fact that they are not polar, the monomeric solubility of nonionic surfactants in general and OG in particular is influenced by ionic strength (Becher, 1967; Shinoda et al., 1961). We have determined the CMC of OG in solutions of various NaCl concentrations by using the fluorescent probe ANS (Fig. 1, *inset*). Fig. 1 shows the evolution of the CMC of OG with the NaCl concentration in the solution. The CMC of OG decreases from 25 mM in pure water to 12 mM in a solution containing 1 M NaCl. These results are in good agreement with those obtained by Shinoda et al. (1961) at [NaCl] of 0.5 M and 1 M, using surface tension measurements.

The solubilization of intact virus by OG was studied by following the evolution of the turbidity signal at 550 nm during the continuous addition of OG to a suspension of VSV. To determine the conditions under which the solubilization process became independent of the rate of OG addition, the experiment was performed at four different rates (6.94 μmol OG/min, 2.78 μmol OG/min, 1.39 μmol OG/min, 0.69 μmol OG/min). We found that the amount of OG required for the total solubilization of the virus was not dependent on the rate of OG addition (data not shown). This indicates that the molecular equilibrium of OG between the solution and the virus or the amphiphile aggregates issued from its solubilization is achieved very rapidly. Our experiments were performed at the slowest rate of OG addition, i.e., 0.69 μmol OG/min (72 min for total solubilization).

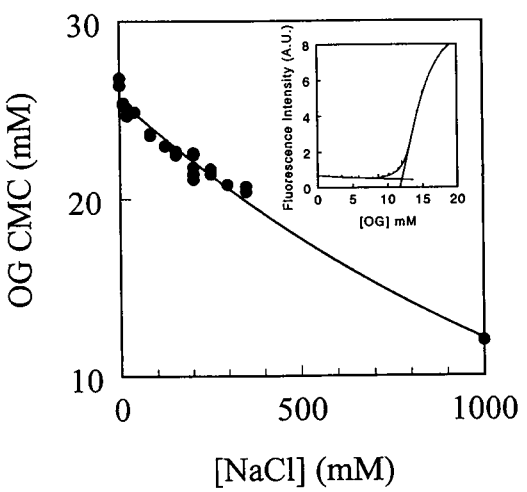

FIGURE 1 CMC of OG as a function of [NaCl]. (*Inset*) ANS fluorescence intensity increase as a function of the OG concentration (T = 25°C). The CMC of OG in the high saline buffer (1 M NaCl, 10 mM HEPES, pH 7.4) is determined at the intercept of the tangents, as indicated on the inset.

In Fig. 2 *A* the solubilization profiles obtained for eight different VSV concentrations are presented. Increasing the initial VSV concentration in the cuvette shifts the solubilization profiles toward higher OG concentration. These curves exhibit reproducible breakpoints, which are determined by the intercept of the tangents, as indicated in Fig. 2 *B*. The total OG concentration ($[OG]_{tot}$) at which those breakpoints are reached shows a linear dependence on the VSV concentration (Fig. 3). Two types of information are provided by the relationships found by linear regression analysis (Ollivon et al., 1988; Paternostre et al., 1988; Meyer et al., 1992; de Foresta et al., 1990; Lichtenberg, 1996):

1. The slopes yield the relative composition of OG in the mixed aggregates (R), which can be expressed as a function of the OG concentration in the aggregates and either the total protein content ($R = [OG]_a/[P]_{tot}$), or the membrane protein content ($R' = [OG]_a/[M\text{-}P + G\text{-}P]$). M-P and G-P are the two membrane proteins of the viral envelope (extrinsic and intrinsic, respectively).

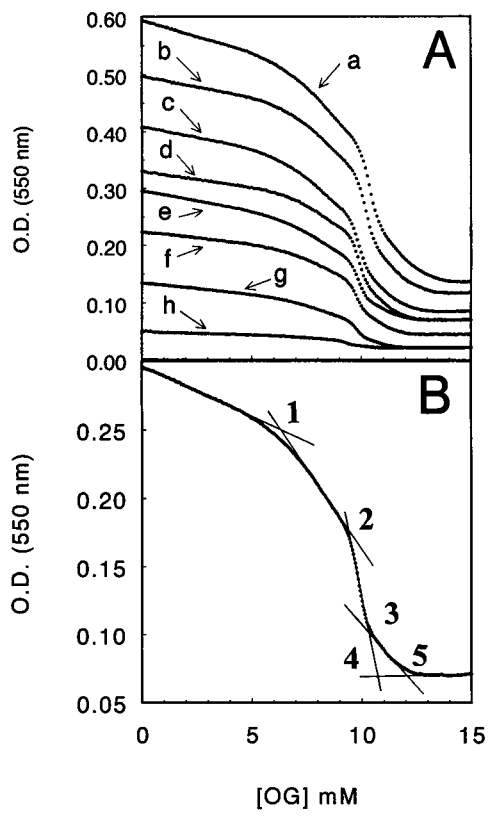

FIGURE 2 Solubilization profiles of VSV by OG obtained by turbidimetric measurement (O.D. at 550 nm) during the continuous addition of OG (addition rate of 0.69 μmol of OG/min) (T = 25°C). (*A*) Curve a: $[VSV]_0$ = 1.13 mg of total protein/ml; curve b: $[VSV]_0$ = 0.96 mg of total protein/ml; curve c: $[VSV]_0$ = 0.80 mg of total protein/ml; curve d: $[VSV]_0$ = 0.59 mg of total protein/ml; curve e: $[VSV]_0$ = 0.57 mg of total protein/ml; curve f: $[VSV]_0$ = 0.39 mg of total protein/ml; curve g: $[VSV]_0$ = 0.28 mg of total protein/ml; curve h: $[VSV]_0$ = 0.07 mg of total protein/ml. (*B*) Graphic determination of breakpoints 1, 2, 3, 4, and 5 from the tangent intercept, as for curve e ($[VSV]_0$ = 0.57 mg of total protein/ml).

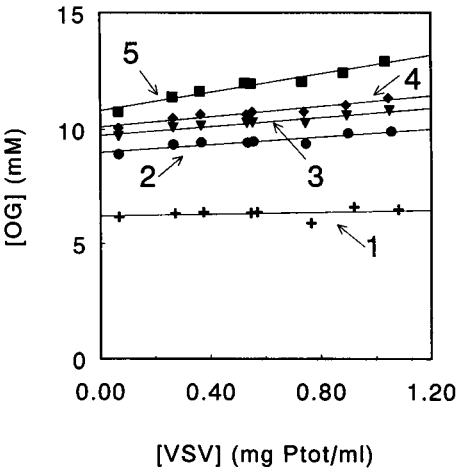

FIGURE 3 Relationships between [OG] and [VSV] at each of the break points indicated on Fig. 2 *B* (see Table 1 for the equations).

2. The intercepts yield the monomeric OG concentration ($[OG]_{mono}$) in equilibrium with the mixed aggregates.

These values are reported for each breakpoint determined for the solubilization profiles in Table 1.

Elimination of the nucleocapsid and characterization of the solubilized material

The [OG] required to solubilize the virus was calculated using Eq. 6, which was deduced from breakpoint 5 of the solubilization profiles (see Table 1):

$$[OG]_{tot} = 10.52 + 1.98 * [P]_{tot}. \quad (6)$$

$[OG]_{tot}$ is expressed in mM, and $[P]_{tot}$ represents the total amount of viral protein (mg/ml).

After OG treatment the viruses were centrifuged at 64,000 × *g* for 1 h to remove the nucleocapsid. SDS-PAGE indicates that the centrifugation results in the total elimination of nucleocapsid, and that all of the G and M proteins remained in the OG extract (Fig. 4).

TABLE 1 Relative composition of the mixed aggregates (R) as a function OG concentration in the aggregates and the protein content ($R = [OG]_a/[P]_{tot}$), or of the OG concentration in the aggregates and the membrane protein content ($R' = [OG]_a/[M\text{-}P + G\text{-}P]$) and monomeric OG concentration ($[OG]_{mono}$) in equilibrium with the mixed aggregates, as determined from the solubilization (breakpoints 1 to 5) and reconstitution (breakpoint 5') profiles

Breakpoints	$[OG]_{mono}$ (mM)	R (mM/(mg/ml))	R' (mM/(mg/ml))
1	6.20	0.2	0.37
2	8.99	0.85	1.57
3	9.74	0.98	1.80
4	10.11	1.11	2.06
5	10.82	1.98	3.66
5'	10.65		3.86

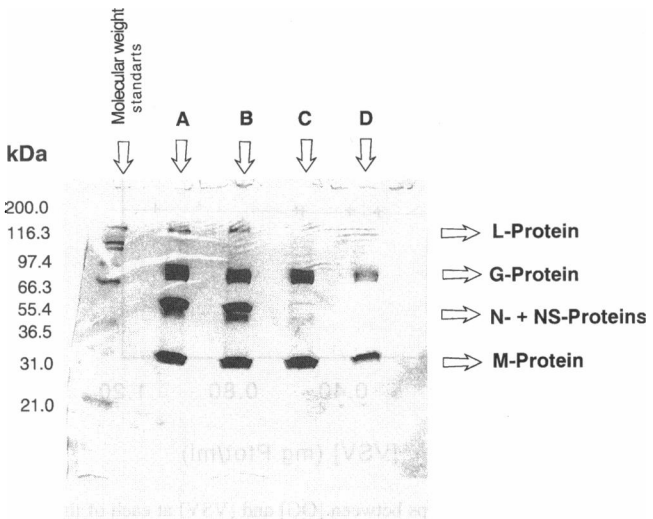

FIGURE 4 SDS-polyacrylamide gel electrophoresis of intact VSV (*A*), of solubilized envelope (*B*), of solubilized envelope after removal of the nucleocapside (*C*), and of reconstituted envelope (after BB SM2 treatment) (*D*).

The amounts of OG, lipid, and protein in the solubilized material were determined by chemical assays and radioactivity measurements of [^{14}C]OG and [^{3}H]leucine before and after centrifugation (Table 2). The concentrations of cholesterol (Chol) on one hand and phosphatidylcholine (PC) and sphingomyeline together on the other were determined in the extracts and compared to their amounts in the membrane of intact VSV, as reported by Pal et al. (1987) (Table 2). According to the literature, these three lipids represent 67% of the total lipid composition of the envelope. The other lipids, phosphatidylserine and phosphatidylethanolamine, which were not assayed, represent 12% and 20%, repectively (mol/mol), of the total lipid content (Pal et al., 1987). Interestingly, after centrifugation, all of the PC, SM, and Chol was recovered, indicating that these lipids were totally solubilized by OG.

The G and M proteins of VSV together represent 55% (w/w) of the total protein and 50% (mol/mol) of the total leucine content of the viral proteins (Pal et al., 1987). SDS-PAGE indicates that after centrifugation, only G and M proteins remained in the supernatant. Chemical analysis of protein concentration indicates that after centrifugation, 53% of the total protein was recovered in the supernatant (Table 2). After centrifugation we also found 50% of the [^{3}H]leucine in the solubilized extract (Table 2). Taken together, these data indicate that 96–100% of G and M proteins was recovered after solubilization.

Measurement of [^{14}C]OG before and after centrifugation demonstrates that the supernatant had the same amount of OG as the initial sample (Table 2). This indicates that the OG interacted with both G and M proteins on one hand and lipids on the other. Moreover, the linear relationship (Eq. 6) determined above allows one to calculate the minimum OG concentration required to fully solubilize the VSV suspension at any concentration of virus, as indicated by the chemical and radioactivity assays performed on the sample after centrifugation. Under these conditions, the detergent extracts all of the lipids of the envelope and the two membrane proteins, i.e., the G protein (which is intrinsic) and the M protein (which is extrinsic).

Reconstitution of the VSV envelope

Because of its high CMC, reconstitution of liposomes and/or proteoliposomes from OG can be achieved by dilution of the solution containing the solubilized material using an OG-free solution. During the dilution procedure, the OG-to-protein and lipid ratio in the aggregates decreased because the quantity of OG in the solution increased. Although by this procedure the detergent is not eliminated

TABLE 2 Characterization of the lipid and protein content of the solubilized virus before and after centrifugation and of the virosomes after BB SM2 treatment, before and after filtration through millipore filters

Assay	VSV composition (Pal et al. 1987)	Before centrifugation	After centrifugation	After BB SM2 treatment	After filtration through millipore filter (0.22 μm)
PC + sphingo (mM)	32% of total lipids*	0.19 mM (100%)¶	0.18 mM (95%)¶	0.10 mM (53%)¶	0.09 mM (47%)¶
Cholesterol (mM)	35% of total lipids*	0.195 mM (100%)‖	0.155 mM (80%)‖	0.105 mM (54%)‖	0.08 mM (41%)‖
P (mg/ml)	G+M = 55% of total Protein#	0.72 mg/ml (100%)#	0.375 mg/ml 53% of P_{tot}# (96% of (G+M)-P#)	0.22 mg/ml 30% of P_{tot}# (55% of (G+M)-P#)	0.175 mg/ml 24% of P_{tot}# 44% of (G+M)-P#
[^{3}H]Leu	G+M = 50% of total [^{3}H]Leuc§	3816 cpm (100% of total [^{3}H]Leuc)§	1909 cpm (50% of total [^{3}H]Leuc§ (100% of (G+M)−P)	1100 cpm (29% of total [^{3}H]Leuc)§ (56% of (G + M)-P)	
[^{14}C]OG		$[OG]_0$ = 14 mM	104% of $[OG]_0$	[OG] = 0.028 mM 0.2% of $[OG]_0$	

*Expressed in mole %.
#Expressed in weight%.
§Expressed in moles of leucine.
¶Expressed in mole % of (PC + Sphin).
‖Expressed in mole % of Chol.

from the sample, the decrease in OG to protein and lipid ratio results in the reconstitution of liposomes. The reconstitution by dilution can be directly monitored by measuring the turbidity of the sample during dilution (Ollivon et al., 1988).

In Fig. 5 we show the profiles obtained during the addition of OG-free buffer to the supernatant obtained after centrifugation of solubilized VSV at different initial concentrations, which contains only the G and M proteins and lipids. These turbidity profiles exhibit a sharp breakpoint, which depends on the concentrations of OG and lipids. This breakpoint is an indication of the beginning of the reconstitution process. Again, the OG concentrations required to reach this point are found to be linearly related to the protein concentrations. From the linear regression analysis we deduced the monomeric concentration of OG ($[OG]_{mono}$) in equilibrium with the aggregates, and the OG-to-membrane protein ratio ([OG]/[G-P + M-P]) in the latter (Table 1). The values determined for these parameters are similar to those determined on the solubilization curves from breakpoint 5, which indicates that the molecular events occurring during the solubilization and the reconstitution are similar. It also indicates that OG does not interact with any component of the nucleocapsid.

Elimination of OG by BB SM2

The reconstitution of virosome as described above involved an important dilution of the sample (final dilution 3.5); the OG is not eliminated by this procedure. To recover fusion activity with more concentrated and OG-free samples, we eliminated OG by using BB SM2. Radiolabeled viruses and OG were used to determine the experimental conditions of OG elimination by following both detergent elimination and possible protein adsorption to the BB SM2. Fig. 6 shows that elimination of the detergent is complete within 120 min after the first addition of BB SM2. At the end of the OG elimination about 40% of the radioactivity corresponding to the [^{3}H]leucine of the M and G proteins was lost on the BB SM2 (see Table 2), together with 50% of PC, Sphyngomyelin, and Chol (see Table 2).

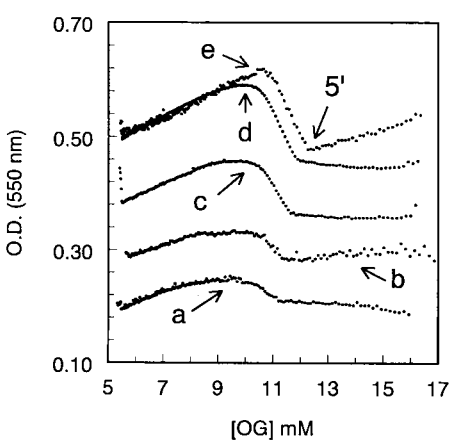

FIGURE 5 (*A*) Reconstitution profiles obtained by turbidity measurements (OD at 550 nm) during the continuous dilution of solubilized VSV (T = 25°C). The initial VSV concentrations are 0.19 mg of (G + M) proteins/ml (*curve a*), 0.29 mg of (G + M) proteins/ml (*curve b*), 0.38 mg of (G + M) proteins/ml (*curve c*), 0.46 mg of (G + M) proteins/ml (*curve d*), and 0.54 mg of (G + M) proteins/ml (*curve e*). The point 5′ is indicated by an arrow on curve e.

Fusion activity of intact viruses and virosomes with Vero cells

To remove large aggregates, the virosomes were filtered through Millipore filters (0.22 μm) before incubation with Vero cells. The filtered samples lost 10–20% of lipid and protein compared to the nonfiltered samples (Table 2). Fig. 7 shows the maximum percentage of fluorescence dequenching for intact viruses and for virosomes as a function of the pH of the solution. The fusion curves described are similar in shape, but the percentage of fluorescence dequenching is about twofold higher for virosomes than for intact viruses. This may be due to the fact that we filtered the virosomes to eliminate aggregates. The fusion of these aggregates would not give an increase in the fluorescence dequenching, but could add to the determination of maximum fluorescence. The pH dependence of fusion is identical for virosomes and viruses. Moreover, antibodies against G-P completely inhibit fusion of virosomes, even at low pH (Table 3). These experiments clearly show that virosomes have an activity similar to that of intact VSV. Moreover, pretreatment of Vero cell-virosome complexes at high tem-

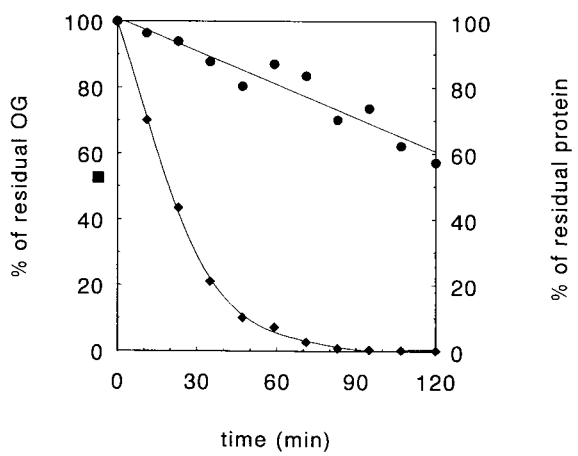

FIGURE 6 Elimination of OG by absorption on BB SM2. The solubilized VSV envelope ([G + M] proteins = 0.44 mg/ml; [OG] = 15 mM) was added to a vial containing 20 mg of wet BB SM2 for each milliliter of sample. The suspension was maintained under continuous magnetic stirring for 12 min. Thereafter the sample was removed from the vials and poured into a new one containing the same amount of BB SM2. These operations were repeated 10 times, and at each step an aliquot of the solution was taken to assay OG (♦) and protein (●). The OG elimination and the protein absorption were followed by radioactivity measurements using [^{14}C]OG- and [^{3}H]leucine-containing proteins. Experiments were performed at room temperature.

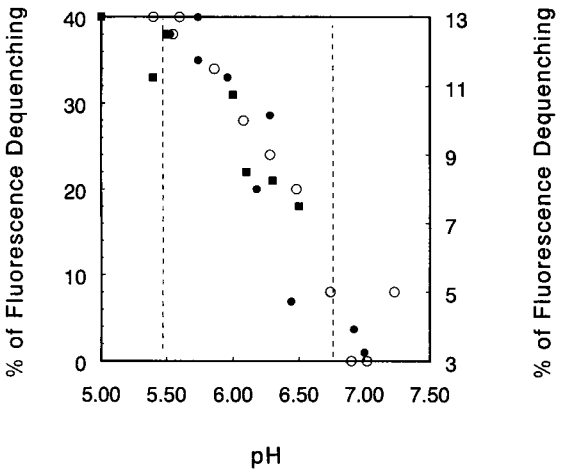

FIGURE 7 pH dependence of fusion. Total extent of fluorescence dequenching as a function of pH, measured from fusion kinetics and realized with intact VSV and Vero cells (○) and with virosomes and Vero cells (●) and (■) for two independent sets of experiments (T = 37°C).

perature or with specific antibody completely inhibited the fusion (see Table 3).

Fusion activity of intact viruses and virosomes with liposomes

Yamada and Ohnishi (1986) measured fusion of VSV with liposomes using spin-labeled lipid. Gaudin et al. (1993) described a procedure to measure the fusogenic activity of rabies virus using liposomes composed of egg phosphatidylcholine, phosphatidylethanolamine, and gangliosides in a weight ratio of 1/2/0.5, respectively. To follow the fusion, they labeled the liposomes with the nonexchangeable fluorescence energy transfer pair NBD-PE and Rho-PE. This composition was optimized by the authors, and fusion activity of intact rabies viruses was measured at 20°C. We used sonicated vesicles of the same composition with an average diameter of about 100 nm, as measured by quasi-elastic light scattering.

Fig. 8 *A* shows the kinetics of virosome fusion at different temperatures and pH 5.8. At 37°C the fluorescence increases rapidly after lowering the pH and thereafter decreases slowly, presumably because of aggregation of virosomes at low pH. The rate of fusion decreased and the extent of fusion increased when the temperature was lowered (Fig. 8 *A*), and no lag times were observed, even at 15°C. In the following experiments the fusion kinetics were recorded at 20°C.

TABLE 3 Inhibition of the fusion activity of virosomes with Vero cells by temperature and antibody pretreatment

Pretreatment	pH	% of fluorescence dequenching
—	7.4	0
—	5.6	17
Antibodies against G-P	5.6	0
High-temperature pretreatment of Vero cell/virosome complexes (56°C, 15 min)	5.6	0

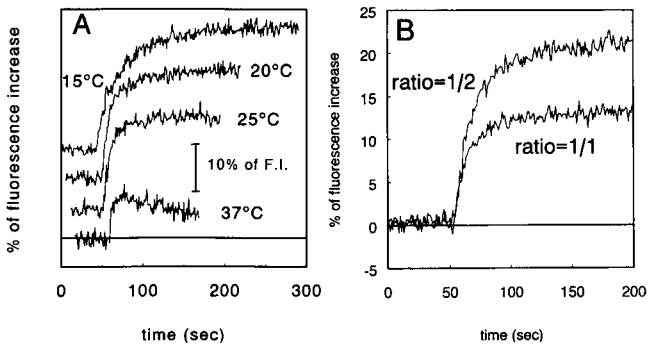

FIGURE 8 Kinetics of fluorescence increase (F.I.) of NBD-PE/Rho-PE-labeled liposomes with intact VSV. (*A*) Fluorescence increase after pH change from 7.4 to 5.8 at different temperatures ranging from 37°C to 15°C. (*B*) Fluorescence increase after pH change for two different liposome/VSV ratios (T = 20°C). Ratio 1/1: 20 μl of labeled liposomes at 1 mg/ml of lipids and 20 μl of VSV at 1 mg of total protein/ml; ratio 1/2: 10 μl of labeled liposomes at 1 mg/ml of lipids and 20 μl of VSV at 1 mg of total protein/ml.

In Fig. 8 *B* the fusion kinetics at two different [liposome]/[virus] ratios are shown. The concentration of virus was kept constant (20 μl of virus at about 1 mg/ml in 2 ml of buffer), and the liposome concentration was changed. The initial rates of the fluorescence increase did not change, but the extent of fluorescence did depend on the liposome concentration, as expected. In the following experiments, a ratio of 2:1 was used to measure fusion kinetics.

Fig. 9 *A* shows the fusion kinetics obtained for intact VSV and NBD-PE/Rho-PE liposomes at 20°C for different pH values. Contrary to the results obtained with rabies virus (Gaudin et al., 1993, 1995b), the fusion kinetics did not show any lag time at any pH. The dependence of fusion activity upon pH is similar to that observed for the fusion of virus with Vero cells (Fig. 9 *C*). The pH threshold is about pH 6.6, which is in good agreement with previously reported results and with results determined from experiments with Vero cells (Fig. 7). However, the pH threshold is more pronounced with liposomes than with Vero cells (the experiments with Vero cells were performed at 37°C). This is probably due to the occurrence of some endocytosis in this last case.

The fusion kinetics recorded between virosomes and liposomes (Fig. 9 *B*) exhibit a pH dependence similar to that obtained in the case of intact viruses (Fig. 9 *C*): a pH threshold at about 6.6/6.7, no lag time, and a fast initial rate of fusion, which also depends on the pH. However, the total fluorescence increase and the initial rate of fluorescence increase are slightly lower for virosomes than for intact virus.

DISCUSSION

The considerations for planning and carrying out the reconstitution of viral proteins into vesicles are very similar to

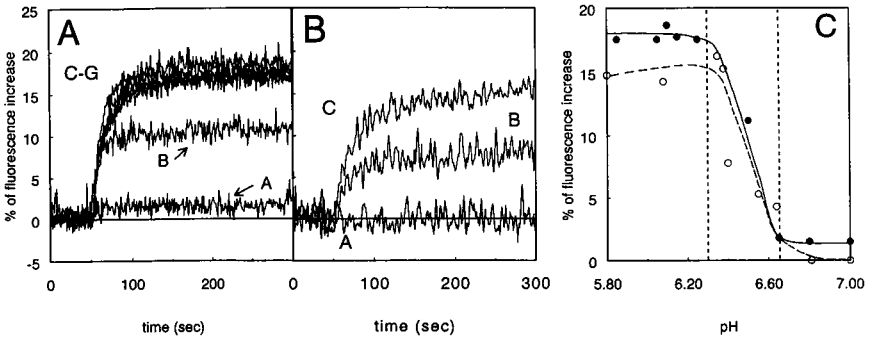

FIGURE 9 (*A*) Kinetics of fluorescence increase (F.I.) of NBD-PE/Rho-PE-labeled liposomes with intact VSV for different pH (20°C). Curve A: pH 6.65; curve B: pH 6.5; curve C-G: 5.85 < pH < 6.25. (*B*) Kinetics of fluorescence increase (F.I.) of NBD-PE/Rho-PE-labeled liposomes with virosomes for different pH (20°C). Curve A: pH 6.81; curve B: pH 6.4; curve C: pH 6.35. (*C*) Total extent of fluorescence increase as a function of pH for intact VSV (●) and for virosomes (○).

those for reconstituting any intrinsic membrane protein. Structurally, viral spike glycoproteins differ from membrane receptor and transport proteins in that the major portion extends into the aqueous phase, with only a small hydrophobic tail in the membrane. This property may affect the reconstitution process simply because both the hydrophilic and hydrophobic regions must be protected from irreversible denaturation throughout the procedure. To be useful, both for practical and for research purposes, reconstituted viral fusion proteins must be able to induce fusion between membranes in a biologically relevant manner. This requires fusion proteins to be anchored and oriented in the reconstituted membrane in a fashion similar to that existing in the original viral envelope.

The concept of reconstitution, when applied to membrane proteins, generally means that the protein in question has been extracted from its native membrane with the aid of a detergent and placed in a newly formed membrane by subsequent removal of this detergent. The solubilized protein is purified (with or without its original lipids) and resituated, alone or in combination with other proteins, in a bilayer composed of native and/or exogenous lipids. It is this ability to recombine the protein in question with other proteins, lipids, and tracers that makes reconstitution so appealing.

Detergents solubilize membranes by intercalating among the phospholipids until the mole fraction of detergent is so high that the mixture no longer forms a bilayer. Evidence for this schema, which may differ in detail among detergents, derives from measurements made as a function of detergent concentration. These include observing the turbidity of aqueous lipid-detergent mixtures (Ollivon et al., 1988; Lesieur et al., 1990; Paternostre et al., 1988), the morphology of particles by electron microscopy (Paternostre et al., 1988; Seras et al., 1996), the distribution of lipids in different environments by ^{31}P NMR (Jackson et al., 1982; Paternostre et al., 1988), the evolution of fluorescence energy transfer between lipidic probes (Ollivon et al., 1988), the evolution of the partition coefficient of the detergents (de Foresta et al., 1990; Paternostre et al., 1995), and the evolution of the relative fluorescence anisotropy of lipidic probes (Jackson et al., 1982) during the solubilization process. The molecular rearrangements that occur during membrane formation, as detergent is removed, follow the same pathway as the solubilization event.

Although a large number of viral spike glycoproteins have been incorporated into lipid vesicles, it has been shown in only a few cases that the reconstituted product was functionally active in the same way as intact virus in inducing membrane fusion. Procedures have been developed for the formation of reconstituted viral envelopes, the fusogenic activity of which was very similar to that of the intact virus. A successful method, first applied to Sendai virus, involves extraction of the envelope by Triton X-100 followed by detergent removal by the direct addition of BB SM2. This method was then successfully applied to influenza virus and VSV. However, it appeared that OG was a poor detergent for reconstitution of viral envelope glycoproteins. Why did we succeed in OG reconstitution where other attempts failed? In most of the cases, a large excess of detergent is added to the membrane suspension to achieve the solubilization of all of the membrane components. However, it is known, at least for mixed lipid-detergent micelles, that the aggregation number of the mixed micelles (and, as a consequence, their sizes) decreases when the quantity of detergent is increased proportionally to the lipid (Eidelman et al., 1988). In the small mixed micelles, water can penetrate because of the very high radius of curvature, and presumably it denatures the protein. A larger micelle would protect the protein from denaturation by aqueous solvent. Moreover, the mixed micellar size can also determine the aggregation state of the G-P. It is known that Triton X-100 forms larger micelles than OG (Kamayama and Takagi, 1990; Yedgar et al., 1974). Wilcox et al. (1992) observed that the G-P trimer was stable in Triton X-100 but unstable in OG. However, in that study VSV was solubilized in 50 mM OG, which is a very high OG concentration compared to that used here. If the functional reconstitution is achieved when the G-P trimer is maintained in the mixed micelles, perhaps the fact that we added the minimum of OG is the crucial reason for this functional reconstitution. Thereafter, we attribute this functional reconstitution from OG to lower amounts of OG used for solubilization. Moreover, the solubilization study allowed us to determine the phase boundaries of this process, particularly the minimum quantity of OG that induces the total solubilization of the viral envelope. The OG-to-total protein ratio at solubilization is about 2 (Fig. 2, Table 1) for a monomeric OG concentration in equilibrium of about 12 mM.

Concerning the other four boundaries determined from the solubilization experiments, these limits correspond to four different and well-defined aggregation states of detergent, lipids, and protein, i.e. from Fig. 3 the [OG]/[protein] ratio in the aggregates and the monomeric [OG] in the solution in equilibrium with the aggregates are known for all of the boundaries determined. However, these aggregates have to be studied to determine the structures and the aggregation numbers associated with them. These boundaries correspond to mixed detergent-protein-lipid membranes, and it will be interesting to determine whether the nucleocapsid can be eliminated from these different mixtures. Indeed, Ollivon et al. (1988) have shown that OG, at sub-solubilizing concentration, formed pores in pure lipidic membrane. If such structures exist as intermediates during the solubilization of natural membranes, they may allow nucleocapsid elimination at a stage where the organization of the membrane is not completely disrupted. Then functional and nicely organized virosomes can perhaps be obtained at least at one of these different boundaries.

Concerning the characterization of the solubilized virus, it appears that OG solubilizes all of the lipids and the two membrane proteins together, i.e., G and M proteins. These two proteins are recovered into the final virosomes after reconstitution. The influence of the M-protein on the reconstitution system is not clear. Lyles et al. (1992) have shown that in vitro M-protein interacts with G-protein. They concluded that these interactions could govern the "in vivo" assembly of the G-protein into the virus envelopes. Then, a possibility could be that, in addition to the conditions of solubilization, the presence of M-protein in our reconstitution helps to maintain the association of G-protein in trimers.

In this work the morphology and the asymmetry of the reconstituted systems were not systematically studied. Concerning the morphology, the virosomes were at least partly aggregated (Table 2), and some improvement in the reconstitution must be found to reduce this perturbing phenomenon. Moreover, because of the procedure (total solubilization of both lipids and proteins followed by detergent removal), the lipids and the proteins were probably randomly oriented in the reconstituted membrane. The fusion activity measured with this system was then only related to the proportion of well-oriented proteins. To achieve an asymmetrical reconstitution of the protein into the liposomes, other reconstitution procedure must be used, particularly direct incorporation into liposomes pretreated with a sub-solubilizing concentration of detergent. However, the aim of this paper was more to determine the solubilization conditions of the VSV membrane proteins by OG without any loss of fusion activity than to perform a well-defined proteoliposome system. This study is the next step to be undertaken in our laboratory.

Finally, the activity and, in particular, the pH dependence of the fusion activity found for the virosomes is similar to that of the virus, whatever the target membrane used (Vero cells or liposomes): in both cases a pH threshold of 6.6/6.7 was found, even if, in the case of NBD-PE and Rho-PE liposomes, the threshold was sharper than in the case of Vero cells. For the fusion assay developed with Vero cells, the virosomes were labeled with R_{18}, and for the assay developed with liposomes, these last were labeled with NBD-PE and Rho-PE. In the first case, the fusion extent was greatly enhanced after virosome filtration, whereas in the second the fusion extent was independent of the filtration. This indicates that the virosomes were at least partly aggregated and that they did not fuse with the target membrane.

The liposomes composed of phosphatidylcholine, phosphatidylethanol amine, and gangliosides have been chosen to study the fusion kinetics of rabies viruses (Gaudin et al., 1993) and were used, in the present work, for the first time to follow VSV and VSV virosome fusion activity. In Fig. 8 *A* the influence of the temperature on the fusion of intact viruses with these liposomes is shown. At 37°C, the initial fusion rate is very fast, but the total extent of fusion is low. Decreasing the temperature induces a decrease in the initial rate and an important increase in the total extent of fusion. This last behavior has also been described by Gaudin et al. (1993) in the case of rabies virus. However, Blumenthal et al. (1987) showed an increase with increasing temperature in the extent of fusion of VSV with Vero cells. Yamada and Ohnishi (1986) showed that the extent of fusion of VSV with 1,2-dioleoyl-*sn*-glycero-3-phosphocholine or phosphatidylcholine and 1,2-dimyristoyl-*sn*-glycero-3-phosphoserine liposomes increased with increasing temperature. In the case of rabies virus (Gaudin et al., 1991, 1993, 1995b), the decrease in fusion extent with increasing temperature was attributed to an increase in the aggregation rate of viruses at the higher temperature. We believe that a similar phenomenon is taking place in our VSV-liposome fusion experiments (Fig. 8 *A*).

Elucidation of molecular mechanisms of viral membrane fusion processes requires the isolation, purification, and functional reconstitution of viral spike glycoproteins. Thus the isolated fusion proteins can be studied in a well-defined lipid environment at controlled surface densities. In addition, in studies on viral fusion and entry into cells, the use of virosomes as a model for the native virus allows the insertion of specific reporter molecules into the membrane or into the aqueous lumen. Fusogenic virosomes provide carrier systems for introducing genetic material into cells. This detailed study on the solubilization and reconstitution of an important viral envelope glycoprotein is a preliminary step in the realization of these goals.

The authors thank Dr. Y. Gaudin for providing them with VSV and for helpful discussions and advice.

This work was supported by PICS CNRS 96, and by the "Ministère de l'Enseignement Supérieur et de la Recherche" (action coordonnée ciblée "Physicochimie des Membranes Biologiques").

REFERENCES

Becher, P. 1967. Micelle Formation in Aqueous and Nonaqueous Solutions. Marcel Dekker, New York.

Blumenthal, R. 1987. Membrane fusion. *Curr. Top. Membr. Transp.* 29: 203–254.

Blumenthal, R., A. Bali-Puri, A. Walter, D. Covell, and O. Eidelman. 1987. pH-dependent fusion of vesicular stomatitis virus with vero cells. *J. Biol. Chem.* 262:13614–13619.

Blumenthal, R., and A. Loyter. 1991. Reconstituted viral envelopes—"Trojan horses" for drug delivery and gene therapy. *Trends Biotechnol.* 9:41–45.

Blumenthal, R., C. C. Pak, M. Krumbiegel, R. J. Lowy, A. Puri, H. F. Elson, and D. S. Dimitrov. 1994. How viral glycoproteins negociate the entry of genetic material into the cell. *In* Biotechnology today. R. Verna and A. Shamoo, editors. Ares Serono Symposia Publications, Rome. 151–173.

Blumenthal, R., D. P. Sarkar, S. Durell, D. E. Howard, and S. J. Morris. 1996. Dilatation of the influenza hemagglutinin fusion pore revealed by the kinetics of individual cell–cell fusion events. *J. Cell. Biol.* 135: 63–71.

Bron, R., A. Ortiz, J. Dijkstra, T. Stegmann, and J. Wilschut. 1993. Preparation, properties and application of reconstituted influenza virus envelopes (virosomes). *Methods Enzymol.* 220:313–331.

Clague, M. J., C. Schoch, L. Zech, and R. Blumenthal. 1990. Gating kinetics of pH-activated membrane fusion of vesicular stomatitis virus with vero cells: stopped flow measurements by dequenching of octadecylrhodamine fluorescence. *Biochemistry.* 29:1303–1308.

de Foresta, B., B. Merah, M. le Maire, and P. Champeil. 1990. How to evaluate the distribution of an invisible amphiphile between biological membranes and water. *Anal. Biochem.* 189:59–67.

Eidelman, O., R. Blumenthal, and A. Walter. 1988. Composition of octyl glucoside-phosphatidylcholine mixed micelles. *Biochemistry.* 27: 2839–2846.

Eidelman, O., R. Schlegel, T. S. Tralka, and R. Blumenthal. 1984. pH-dependent fusion induced by vesicular stomatitis virus glycoprotein reconstituted into phospholipid vesicles. *J. Biol. Chem.* 259:4622–4628.

Eytan, G. D. 1982. Use of liposomes for reconstitution of biological functions. *Biochim. Biophys. Acta.* 694:185–202.

Gaudin, Y., R. W. H. Ruigrok, and J. Brunner. 1995a. Low-pH induced conformational changes in viral fusion proteins—implications for the fusion mechanism. *J. Gen. Virol.* 76:1541–1556.

Gaudin, Y., R. W. H. Ruigrok, and J. Brunner. 1995b. Low-pH induced conformational changes in viral fusion proteins: implications for the fusion mechanism. *J. Gen. Virol.* 76:1541–1556.

Gaudin, Y., R. W. H. Ruigrok, M. Knossov, and A. Flamand. 1993. Low pH conformational changes of rabies virus glycoprotein and their role in membrane fusion. *J. Virol.* 67:1365–1372.

Gaudin, Y., C. Tuffereau, D. Segretain, M. Knossow, and A. Flamand. 1991. Reversible conformational changes and fusion activity of rabies virus glycoprotein. *J. Virol.* 65:4853–4859.

Hoekstra, D., T. de Boer, K. Klappe, and J. Wilschut. 1984. Fluorescent method for measuring the kinetics of fusion between biological membranes. *Biochemistry.* 23:5675–5681.

Hug, P., and R. G. Sleight. 1994. Fusogenic virosomes prepared by partitioning of vesicular stomatitis virus G protein into preformed vesicles. *J. Biol. Chem.* 269:4050–4056.

Jackson, M. L., C. F. Schmidt, D. Lichtenberg, B. J. Litman, and A. D. Albert. 1982. Solubilization of phosphatidylcholine bilayers by octyl glucoside. *Biochemistry.* 21:4576–4582.

Kamayama, K., and T. Takagi. 1990. Micellar properties of octyl glucoside in aqueous solutions. *J. Colloid Interface Sci.* 137:1–10.

Lapidot, M., O. Nussbaum, and A. Loyter. 1987. Fusion of membrane vesicles bearing only with influenza hemagglutinin with erythrocytes, living cultured cells and liposomes *J. Biol. Chem.* 262:13736–13741.

Lenard, J. 1990. Membrane fusion and the infectious entry of viruses into cells. *In* Membrane Fusion. J. W. Wilschut and D. Hoekstra, editors. Marcel Dekker, New York. 275–289.

Lesieur, S., C. Grabielle-Madelmont, M.-T. Paternostre, J. M. Moreau, R. M. Handjani-Villa, and M. Ollivon. 1990. Action of octylglucoside on non-ionic monoalkyl amphiphile-cholesterol vesicles: study of the solubilization mechanism. *Chem. Phys. Lipids.* 56:109–121.

Lichtenberg, D. 1996. Liposomes as a Model for Solubilization and Reconstitution of Membranes. CRC Press, Boca Raton, FL.

Lorge, P., V. Cabiaux, L. Long, and J. H. Ruysshaert. 1986. Fusion of newcastle disease virus with liposomes: role of the lipid composition of liposomes. *Biochim. Biophys. Acta.* 858:312–316.

Lyles, D. S., M. McKenzi, and J. W. Parce. 1992. Subunit interactions of vesicular stomatitis virus envelope glycoprotein stabilized by binding to viral matrix protein. *J. Virol.* 66:349–358.

Marsh, M., and A. Helenius. 1989. Virus entry into animal cells. *Adv. Virus Res.* 36:107–151.

Metsikkö, K., G. Van Meere, and K. Simons. 1986. Reconstitution of the fusogenic activity of vesicular stomatitis virus. *EMBO J.* 5:3429–3435.

Meyer, O., M. Ollivon, and M. Paternostre. 1992. Solubilization steps of dark-adapted purple membrane by Triton X-100: a spectroscopic study. *FEBS Lett.* 305:249–253.

Miller, D. K., B. I. Feuer, R. Vanderoef, and J. Lenard. 1980. Reconstituted G protein-lipid vesicles from vesicular stomatitis virus and their inhibition of VSV infection. *J. Cell Biol.* 84:421–429.

Newcomb, W. W., G. J. Tobin, J. J. McGowan, and J. C. Brown. 1982. In vitro reassembly of vesicular stomatitis virus skeletons. *J. Virol.* 41: 1055–1062.

Nussbaum, O., M. Lapidot, and A. Loyter. 1987. Reconstitution of functional influenza virus envelopes and fusion with membranes and liposomes lacking virus receptors. *J. Virol.* 61:2245–2252.

Ollivon, M., O. Eidelman, R. Blumenthal, and A. Walter. 1988. Micelle-vesicle transition of egg phosphatidylcholine and octyl glucoside. *Biochemistry.* 27:1695–1703.

Pal, R., Y. Barenholz, and R. R. Wagner. 1987. Vesicular stomatitis virus membrane proteins and their interactions with lipid bilayers. *Biochim. Biophys. Acta.* 906:175–193.

Pal, R., J. R. Wiener, Y. Barenholz, and R. R. Wagner. 1983. Influence of the membrane glycoprotein and cholesterol of vesicular stomatitis virus on the dynamics of viral and model membranes: fluorescence studies. *Biochemistry.* 22:3624–3630.

Paternostre, M.-T., R. J. Lowy, and R. Blumenthal. 1989. pH-Dependent fusion of reconstituted vesicular stomatitis virus envelopes with Vero cells. Measurement by dequenching of fluorescence. *FEBS. Lett.* 243: 251–258.

Paternostre, M., O. Meyer, C. Grabielle-Madelmont, S. Lesieur, M. Ghanam, and M. Ollivon. 1995. Partition coefficient of a surfactant between aggregates and solution: application to the micelle-vesicle transition of egg-phosphatidylcholine and octylglucoside. *Biophys. J.* 69:2476–2488.

Paternostre, M.-T., M. Roux, and J.-L. Rigaud. 1988. Mechanisms of membrane protein insertion into liposomes during reconstitution procedures involving the use of detergents. 1. Solubilization of large unilamellar liposomes (prepared by reverse-phase evaporation) by Triton X-100, octyl glucoside and sodium cholate. *Biochemistry.* 27: 2668–2677.

Petri, W. A. J., and R. R. Wagner. 1979. Reconstitution into liposomes of the glycoprotein of vesicular stomatitis virus by detergent dialysis. *J. Biol. Chem.* 254:4313–4316.

Petri, W. A. J., and R. R. Wagner. 1980. Glycoprotein micelles isolated from vesicular stomatitis virus spontaneously partition into sonicated phosphatidylcholine vesicles. *Virology.* 107:543–547.

Puri, A., M. Clague, C. Schloch, and R. Blumenthal. 1993a. Kinetics of fusion of enveloped viruses with cells. *Methods Enzymol.* 220:227–287.

Puri, A., D. S. Dimitrov, H. Golding, and R. Blumenthal. 1992a. Interactions of CD4+ plasma membrane vesicles with HIV-1 and HIV-1 envelope glycoprotein-expressing cells. *J. Acquir. Immune Defic. Syndr.* 5:915–920.

Puri, A., S. Grimaldi, and R. Blumenthal. 1992b. Role of viral envelope sialic acid in membrane fusion mediated by the vesicular stomatitis virus envelope glycoprotein. *Biochemistry.* 31:10108–10113.

Puri, A., M. Krumbiegel, D. Dimitrov, and R. Blumenthal. 1993b. A new approach to measure fusion activity of cloned viral envelope proteins: fluorescence dequenching of octadecylrhodamine-labelled plasma mem-

brane vesicles fusing with cells expressing vesicular stomatitis virus glycoprotein. *Virology.* 195:-858.

Rigaud, J.-L., M.-T. Paternostre, and A. Bluzat. 1988. Mechanisms of membrane protein insertion into liposomes during reconstitution procedures involving the use of detergents. 2. Incorporation of the light-driven proton pump bacteriorhodopsin. *Biochemistry.* 27:2677–2688.

Rigaud, J. L., B. Pitard, and D. Levy. 1995. Reconstitution of membrane proteins into liposomes: application to energy transducing-membrane proteins. *Biochim. Biophys. Acta.* 1231:223–246.

Sarkar, D. P., S. J. Morris, O. Eidelman, J. Zimmerberg, and R. Blumenthal. 1989. Initial stages of influenza hemagglutinin-induced cell fusion monitored simultaneously by two fluorescent events: cytoplasmic continuity and lipid mixing. *J. Cell. Biol.* 109:113–122.

Schoch, C., and R. Blumenthal. 1993. Role of the fusion peptide sequence in initial stages of influenza hemagglutinin-induced cell fusion. *J. Biol. Chem.* 268:9267–9274.

Seras, M., K. Edwards, M. Almgren, G. Carlson, M. Ollivon, and S. Lesieur. 1996. Solubilization of non-ionic monoalkyl amphiphile-cholesterol by octyl glucoside: cryo-transmission electron microscopy of the intermediate structures. *Langmuir.* 12:330–336.

Shinoda, K., T. Yamaguchi, and R. Hori. 1961. The surface tension and the critical micelle concentration in aqueous solution of β-D-alkyl glucosides and their mixtures. *Bull. Chem. Soc. Jpn.* 34:237–241.

Stegmann, T., H. W. Morselt, F. P. Booy, J. F. Van Breenen, G. Scherphof, and J. Wilschut. 1987. Functional reconstitution of influenza virus envelopes. *EMBO J.* 6:2651–2659.

Stegmann, T., S. Nir, and J. Wilschut. 1989. Membrane fusion activity of influenza virus: effect of gangliosides and negatively charged phospholipids in target liposomes. *Biochemistry.* 28:1698–1704.

Struck, D. K., D. Hoekstra, and R. E. Pagano. 1981. Use of resonnance energy transfer to monitor membrane fusion. *Biochemistry.* 20: 4093–4099.

Vainstein, A., H. Herhokovitz, S. Israel, S. Rabin, and A. Loyter. 1984. A new method for reconstitution of highly fusogenic Sendai virus envelopes. *Biochim. Biophys. Acta.* 773:181–188.

Walter, A., O. Eidelman, M. Ollivon, and R. Blumenthal. 1988. Functional reconstitution of viral envelopes. *In* Membrane Fusion. J. W. Wilschut and D. Hoekstra, editors. Marcel Dekker, New York. 395–420.

White, J. M. 1992. Membrane fusion. *Science.* 258:917–924.

Wilcox, M. D., M. O. McKenzie, J. W. Parce, and D. S. Lyles. 1992. Subunit interactions of vesicular stomatitis virus envelope glycoprotein influenced by detergent micelles and lipid bilayers. *Biochemistry.* 31: 10458–10464.

Wilschut, J., J. Cower, J. L. Nieva, R. Bron, L. Moesby, R. C. Reddy, and R. Bittman. 1995. Fusion of Semliki forest virus with cholesterol-containing liposomes at low pH: a specific requirement of sphingolipids. *Mol. Membr. Biol.* 12:143–149.

Yamada, S., and S. Ohnishi. 1986. Vesicular stomatitis virus binds and fuses with phospholipid domains in target cell membranes. *Biochemistry.* 25:3703–3708.

Yedgar, S., Y. Barenholz, and V. G. Cooper. 1974. Molecular weight, shape and structure of mixed micelles of Triton X-100 and sphingomyelin. *Biochim. Biophys. Acta.* 363:98–111.

Zimmerberg, J., R. Blumenthal, D. P. Sarkar, M. Curran, and S. J. Morris. 1994. Restricted movement of lipid and aqueous dyes through pores formed by influenza hemagglutinin during cell fusion. *J. Cell. Biol.* 127:1885–1894.